Utah NASA Space Grant Consortium Fellowship Symposium Proceedings
May 2019

Administering Model-based Patient-specific Supplemental Oxygen Therapy

Kyle M. Burk[1,2]
Joseph A. Orr[1,2]

Abstract *Purpose:* The oxyhemoglobin dissociation curve describes the relationship between the partial pressure of oxygen and the percent of hemoglobin saturated with oxygen and varies with chemical and physical factors that differ for every patient. If variability could be determined, patient specific oxygen therapy could be administered. We have developed a procedure for characterizing variations in the oxygen dissociation curve. The purpose of this study was to validate this procedure in surgical patients. *Methods:* The procedure uses an automated system to alter oxygen therapy and Hill's equation to fit measurements. Once measurements are gathered, the procedure uses an iterative least-squares method to determine best-fit parameters for the Hill equation. The procedure was performed on surgical patients after which model fit was assessed. *Results:* 39 patients participated in this study. Using patient-specific parameter values increases correlation when compared to standard values. The procedure improved the model fit of patient saturation values significantly in 19 patients. *Conclusions:* This paper has demonstrated a procedure for determining patient-specific pulse oximeter response. This procedure determined best-fit parameters resulting in a significantly improved fit when compared to standard values. These best-fit parameters increased the coefficient of determination R^2 in all cases.

Keywords Subject-specific modeling · Non-linear least-squares · Oxygen saturation response · The Hill equation

1. Department of Biomedical Engineering, University of Utah, Salt Lake City, UT 84132, USA
2. Department of Anesthesiology, University of Utah, Salt Lake City, UT 84132, USA.

1 Introduction

The oxyhemoglobin dissociation curve (ODC) describes the relationship between the percent of hemoglobin saturated with oxygen (SHbO2) and the partial pressure of oxygen (PO2) in the blood [12,7,15,6,8]. Due to the allosteric effects of oxygen binding with hemoglobin's four oxygen binding sites, this response is a sigmoidal curve [13,3]. Due to hemoglobin's affinity for oxygen, this sigmoid relationship plateaus at a PO2 of approximately 150 mm Hg in healthy patients [12]. Above 150 mm Hg the majority of hemoglobin binding sites are fully saturated with oxygen, and thus SHbO2 is minimally responsive to changes in PO2 while below 150 mm Hg SHbO2 is highly responsive to changes in PO2 [1]. These characteristics of oxyhemoglobin's response to PO2 permit oxygen uptake in the lungs, at high PO2, and oxygen unloading near tissue, at low PO2, and are vital to oxygen transport in the body [9].

Besides oxygen, hemoglobin is responsive to other notable allosteric effectors [7,17,19,20]. These include chemical factors in the blood such as hydrogen ions (pH), carbon dioxide (CO2), and 2,3-Diphosphoglycerate (2,3-DPG) [5]. Hemoglobin's allosteric effectors also include the physical factor of temperature (T). Although the effects of factors are well characterized, the values of the factors are not clinically available in many patients. Patient to patient variation in the concentrations and levels of these effectors, in turn, can effect hemoglobin's affinity for oxygen. Differences in oxygen affinity can affect the position and shape of the ODC, with increased oxygen affinity shifting the curve to the left (lower PO2) and decreased affinity shifting the curve to the right [12]. Thus, hemoglobin's affinity for oxygen varies from patient to patient [18].

Variations in oxygen affinity change the shift and shape of the ODC, including the PO2 at which the

ODC transitions from a plateau to a steep slope. This patient-to-patient variability impacts the level of oxygen therapy required to prevent desaturation. However, if a patient-specific ODC could be generated, the transition from the plateau to sharp curve could be characterized, and patient-specific oxygen therapy could be administered, preventing desaturation. One possibility for determining patient variability is to create an automated procedure which uses a set of PO2 and pulse oxygen saturation (SpO2) value pairs to fit a patient-specific ODC. We have developed such a procedure which is based on an automated oxygen delivery system and Hill's equation.

The procedure measures several levels of oxygen saturation by varying oxygen therapy using an automated system. Best-fit parameters (P_{50}, n, K) for corresponding saturation and oxygen measurements are then found using an iterative minimal least-squares technique. Once these parameters are found, the procedure constructs a patient-specific ODC from which important characteristics, including the transition from the plateau to the steep slope of the curve, can be obtained. Extrapolation of the ODC could also be used to predict a patient-specific response to different levels of oxygen therapy.

The objective of this study was to validate the procedure for determining patient-specific pulse oxygen saturation response. If validated, the procedure could characterize patient-specific oxyhemoglobin using an automated system and non-invasive techniques.

2 Methods

This study was performed in accordance with the 1964 Helsinki declaration and its later amendments or comparable standards. Study approval came from the University of Utah Institutional Review Board. All patients participated with written informed consent.

2.1 Procedure for characterizing oxygen saturation response

The procedure for characterizing pulse oxygen saturation response uses an automated system to alter oxygen therapy to generate patient-specific oxygen flow and saturation data pairs. Hill's equation is then used to characterize the data set for each patient. To determine oxygen saturation response, the automated system administers different levels of oxygen therapy gathering measurements for oxygen and saturation levels at each level. The procedure then uses iterative least squares residual techniques to find the best-fit curve for the gathered measurements.

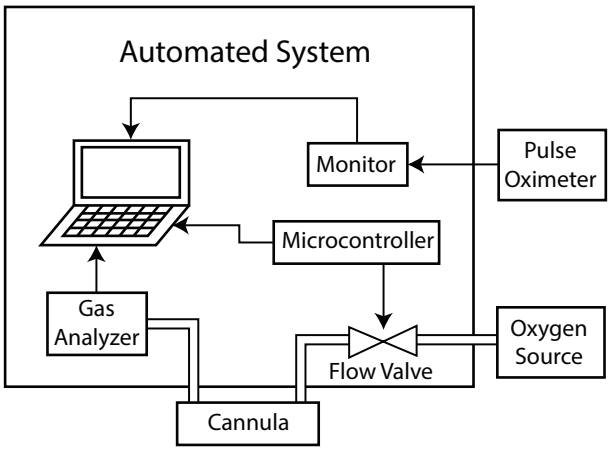

Fig. 1 Schematic diagram of the automated system

2.1.1 Automated oxygen therapy system

Figure 1 shows a schematic diagram of the automated oxygen therapy system which includes a laptop computer. The automated system varies oxygen flow rate using a proportional solenoid valve (MD PRO, Parker Hannifin, Hollis, NH) connected to a compressed oxygen source. A laptop computer collects end-tidal oxygen (etO2) measurements from a gas analyzer (CapnoMAC, Datex, Helsinki, Finland). The laptop computer also collects SpO2 from a pulse oximeter (LNCS^{TM}, Masimo, Irvine, CA). The system monitored nasal pressure to determine breath phase, and discontinued oxygen flow during exhalation so that etO2 measurements were not contaminated by supplemental oxygen.

2.1.2 Theoretical aspects

While varying oxygen, the procedure collects pairs of etO2 and SpO2 measurements. Since the system varies oxygen, a range of SpO2 measurements can be measured to characterize a patient's ODC. After collecting pairs of measurements, the procedure fits the data to Hill's equation:

$$SHbO2 = f(PO2) = K\frac{(PO2/P_{50})^n}{1 + (PO2/P_{50})^n}, \quad (1)$$

where P_{50} is the $PO2$ at which 50% of hemoglobin are saturated with oxygen ($SHbO2 = 50\%$), n is the Hill coefficient, and K is the maximum saturation possible.

Hill's Equation can be used to calculate SHbO2 for any given PO2. Its three variables can be used to determine ODC shift (P_{50}), slope (n), and offset (K). The value of these three variables depends on the conformation of hemoglobin and thus varies between patients.

2.1.3 Determining the best-fit parameters

The procedure finds the best fit P_{50}, n, and K values for each volunteer using iterative non-linear least-squares fitting as implemented in the *least_squares* function of the *optimize* module in *SciPy* (SciPy, v1.1.0, The SciPy community) [14].

The solution to a non-linear least-squares problem is a local minimizer of the problem:

$$\min\{\sum_{i=1}^{m} f_i(x)^2\}, \tag{2}$$

where m is the number of residuals [2]. For analyzing pulse oxygen saturation response, the problem is of the form:

$$f_i(\mathbf{x}) = K\frac{(PO2_i/P_{50})^n}{1+(PO2_i/P_{50})^n} - SpO2_i, \tag{3}$$

where $PO2_i$ (independent) and $SpO2_i$ (dependent) are the ith measured SpO2 and etO2 points, respectively. The patient-specific parameters are contained in $\mathbf{x} = \{P_{50}, n, K\}$. The Jacobian matrix, which is helpful for computing the minimization problem, can be found using the following equations:

$$J_{i0} = \frac{\partial f_i}{\partial P_{50}} = -\frac{Kn}{P_{50}}\frac{(PO2_i/P_{50})^n}{[1+(PO2_i/P_{50})^n]^2} \tag{4}$$

$$J_{i1} = \frac{\partial f_i}{\partial n} = K\log(PO2_i/P_{50})\frac{(PO2_i/P_{50})^n}{[1+(PO2_i/P_{50})^n]^2} \tag{5}$$

$$J_{i2} = \frac{\partial f_i}{\partial K} = \frac{(PO2_i/P_{50})^n}{1+(PO2_i/P_{50})^n} \tag{6}$$

where log is the natural logarithm and values in $\mathbf{x}$ are all positive. The constraints for $\mathbf{x}$ are shown in Table 1.

2.1.4 Estimating oxygen saturation

After the best-fit parameters have been determined using the methods described in Section 2.1.3, the procedure proceeds by estimating oxygen saturation. This is done using the best-fit parameters, etO2 values, and Equation (1). End-tidal oxygen values are converted to PO2 by compensating for local atmospheric pressure (640 mm Hg) and the partial pressure of water vapor at 37^o C (47 mm Hg):

$$PO2 = (640-47)\frac{etO2}{100\%}\text{mm Hg} \tag{7}$$

Table 1 Constraints for $\mathbf{x} = \{P_{50}, n, K\}$

Parameter	Range	Units
P_{50}	15 - 75	mm Hg
n	1.5 - 3.9	unitless
K	0.94 - 1.0	unitless

2.2 Model fit assessment

Model fit assessment methods can be used to quantify how well the model performs. These assessment methods analyze how well the model describes data (descriptive error) and how well it predicts data (predictive error). For modeling oxygen saturation response, model description and prediction error can be analyzed to validate the ability of the procedure to fit and predict SpO2.

Descriptive error can be determined by calculating the coefficient of determination R^2:

$$R^2 = 1 - \frac{\sum_{i=1}^{n}(y_i - f(x_i))^2}{\sum_{i=1}^{n}(y_i - \overline{y})^2}, \tag{8}$$

where f is the Hill equation with best-fit parameters for the particular data set $\mathbf{x}$, $f(x_i)$ represents model estimates computed using f and x_i, y_i are observed measurements, and $\overline{y}$ is the mean of all the y_i measurements:

$$\overline{y} = \frac{1}{n}\sum_{i=1}^{n} y_i \tag{9}$$

Leave-one-out cross-validation can be performed by calculating the predictive coefficient of determination Q^2:

$$Q^2 = 1 - \frac{\sum_{i=1}^{n}(y_i - f_{(-i)}(x_i))^2}{\sum_{i=1}^{n}(y_i - \overline{y})^2}, \tag{10}$$

where $f_{-i}(x_i)$ represents the value at x_i produced when the best-fit parameters were calculated by leaving out x_i. Cross-validation calculates Q^2 by using Equation (10) to loop through each measurement for a given data set, leaving out one data point each time, using the remaining data points to determine the best fit model parameters, and using those best-fit parameters to predict the point left out.

2.3 Study setup and protocol

Participants were selected from surgical patients at the University of Utah Moran Eye Center. Potential participants were selected by a chart review before surgery. Eligible participants had an adult American Society of Anesthesiologists physical status of I-III and were aged

> 18 yr. Patients with a baseline SpO2 $\leq$ 93% on room air, surgery scheduled for less than 20 minutes, ARDS, lung disease, cardiovascular disease, or pregnancy were not eligible to participate.

Before the surgery, participants were fitted with a sampling nasal cannula and the automated system's pulse oximeter. The sampling line of the nasal cannula was connected to the system's gas analyzer. During the procedure, the automated system administered oxygen at varying flow rates. Each flow rate was administered for two minutes after which etO2 and SpO2 were recorded. Given that surgery time would vary between patients we expected to acquire a different number of paired measurements for each patient. Once the surgery concluded and all paired measurements for a patient were collected data analysis proceeded as described in Sections 2.1.3 and 2.1.4. Once best-fit parameters had been determined and oxygen saturation estimated model fit was assessed as described in Section 2.2. For comparison, fit for a model using generic parameter values, $\mathbf{x} = \{26.8, 2.7, 1.0\}$, was also assessed using Equation 8.

2.4 Statistical analysis

Statistical analysis was performed using Python (v2.7.14, Python Software Foundation, Beaverton, OR). Median R^2 and Q^2 across all patients was calculated. The interquartile range (IQR), including 25th and 75th percentiles, was used to report uncertainty.

Differences between measurements y_i and model output $f(x_i)$ were compared for both descriptive and predictive modeling using limits of agreement (LoA) methods. The absolute difference between measurements y_i and model output $f(x_i)/f_{(-i)}(x_i)$ is the residual and was calculated for all measurements:

$$f(x_i) - y_i \tag{11}$$

$$f_{(-i)}(x_i) - y_i \tag{12}$$

LoA methods calculated the mean difference of all data points using (11) or (12). 95% LoA were calculated as ± 1.96 SD where SD is the standard deviation of the difference between all data points. To determine differences between predictive and descriptive modeling, the LoA for descriptive and predictive modeling were compared.

For each patient an F-test was used to determine if the specific fit improved model-fit significantly compared to a standard ODC. The F-statistic F was calculated as:

Table 2 Median and dispersion of optimal values for P_{50}, n, and K

Parameter	Mean (SD)	Range (Min. - Max.)	Units
P_{50}	32.0 (14.4)	53.4 (15.0 - 68.4)	mm Hg
n	3.2 (0.8)	2.2 (1.67 - 3.9)	unitless
K	1.00 (0.01)	0.06 (0.94 - 1.00)	unitless

$$F = \frac{\left(\frac{RSS_{std} - RSS_{spec}}{p_{spec} - p_{std}}\right)}{\left(\frac{RSS_{spec}}{n - p_{spec}}\right)}, \tag{13}$$

where RSS_{std} and RSS_{spec} are the residual sum of squares (RSS) when using the standard and specific curves respectively, $p_{std} = 0$ and $p_{spec} = 3$ are the number of parameters in the standard and specific models respectively, and n is the number of data points. The specific model fit was significantly improved if F calculated using (13) was greater than the critical value of the F-distribution with ($p_{spec} - p_{std}$,$n - p_{spec}$) degrees of freedom and $\alpha = 0.05$.

3 Results

39 patients participated in this study. 498 data points were evaluated with an average of 12 data points per patient. The median values as well as standard deviation (SD) and range for P_{50}, n, and K are shown in Table 2. For 19 of the 39 patients, a specific ODC improved model-fit significantly ($F > F$-critical).

Figure 2 shows the model fit for a typical patient. The best fit parameters for this particular patient were $\mathbf{x} = \{24.9, 1.9, 0.99\}$. When performing leave-one-out analysis, the mean $\pm$ SD for the best fit parameters was $\mathbf{x} = \{25.0 \pm 1.6, 1.9 \pm 0.1, 0.99 \pm 0.001\}$. Using a patient-specific ODC to fit patient data points increased correlation (R^2 : 0.94 vs. -2.36, specific vs. generic) and improved model fit significantly ($F > F$-critical). Leave-one-out analysis also showed increased correlation ($Q^2 = 0.92$). This patient-specific curve shows how oxygen saturation would begin to drop long before a standard ODC would predict. For example, oxygen saturation at 70 mm Hg for the standard curve is 0.93 while for the patient-specific curve it is 0.87.

The coefficient of determination R^2 for all patients are shown in Figure 3. Using patient-specific parameter values resulted in increased correlation compared to standard values (median (IQR) R^2: 0.42 (0.63) vs. -0.22 (2.08), specific vs. standard). The median difference (specific - standard) in R^2 for paired data was 0.85 with an interquartile range from 0.29 to 1.90. The median absolute difference between modeled data points

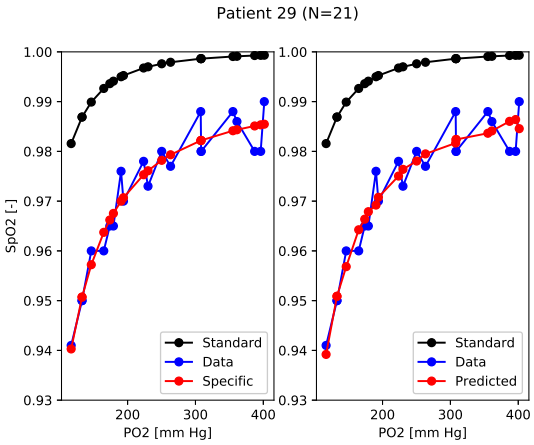

Fig. 2 Model fit and prediction for a select patient. For this particular patient, the best fit values were $\mathbf{x} = \{24.9, 1.9, 0.99\}$. Correlation increased when using a specific oxyhemoglobin dissociation curve (R^2: 0.94 vs. -2.36, specific vs. standard). Leave-one-out analysis also showed increased correlation ($Q^2 = 0.92$)

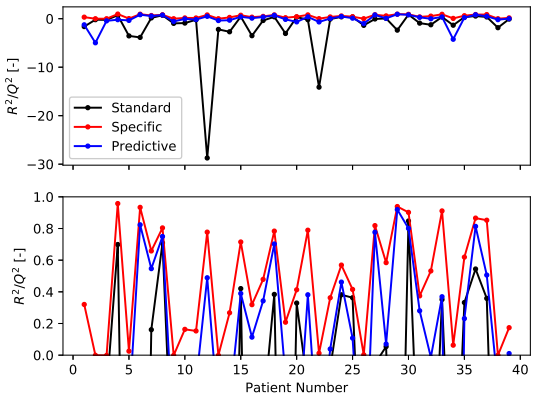

Fig. 3 Coefficient of determination R^2/Q^2 when model parameters are set to standard values compared to when model parameters are set to best-fit values. The upper panel shows an expanded view of all R^2/Q^2 values while the lower panel shows a magnified view centered on the R^2/Q^2 range from 0 to 1

$f(x_i)$ and observed measurements y_i for all patients was -0.0005 SpO2. The 95% LoA were from -0.0149 to 0.0140 SpO2 (Figure 4).

The predictive coefficient of determination Q^2 for all patients are shown in Figure 3. The median (IQR) Q^2 was 0.07 (0.81). The median absolute difference between predicted data points $f_{(-i)}(x_i)$ and observed measurements y_i for all patients was -0.0005 SpO2. The 95% LoA were from -0.0189 to 0.0179 SpO2 (Figure 4).

4 Discussion

This manuscript describes a procedure for determining a patient-specific pulse oxygen saturation response. Results have shown that the procedure improved the model fit of patient saturation values significantly in 19 of 39 patients. Results have also shown that using patient-specific parameter values increases correlation when compared to standard values. The predictive capability of the procedure was also tested, and results show that the LoA when predicting were within ± 0.02 SpO2.

These results demonstrate the ability of the procedure to provide a more accurate estimate of patient oxygen saturation response when compared with using standard parameter values. This accurate estimate could help determine a patient's specific response and thus define the PO2 at which a patient's SpO2 would begin to decline rapidly. Further, this accurate estimate could be used to describe the decline in SpO2 with time.

Previous related research has studied how accurately SpO2 predicts arterial partial pressure of oxygen (PaO2) [4,11]. Brockway *et al.* found that PaO2 correlated significantly with SpO2. This research has added to these results by demonstrating increased correlation when determining patient-specific parameter values.

As expected, the mean best-fit values for model parameters (Table 2) compared well with typical standard values. However, a wide range of parameter values was observed when considering the patient population as a whole. This wide range demonstrates the utility in determining patient-specific parameter values to predict oxygen saturation response.

For some of the parameters, the upper or lower parameter constraint was reached in at least one patient. Two bounds of particular interest for which this occurred were the lower bound of P50=15 and the upper bound of $n = 3.9$. Had the constraint window for these parameters been broader correlation may have been improved but the parameter value may not have been physiologically realistic. This demonstrates the balance between improved model fit and physiologically realistic results. The proper range for realistic constraint windows on P50, n, and K should be explored further and considered in future research on oxygen saturation response.

When predicting SpO2, as simulated using leave-one-out cross-validation, this procedure exhibited larger LoA compared to descriptive modeling. This result indicates that the predictive capability of the procedure depends on the number of measurements acquired, with the predictive capability of the procedure increasing with the number of measurements. Therefore, the number of measurements acquired may influence the accuracy of the procedure's predictions and thus the proce-

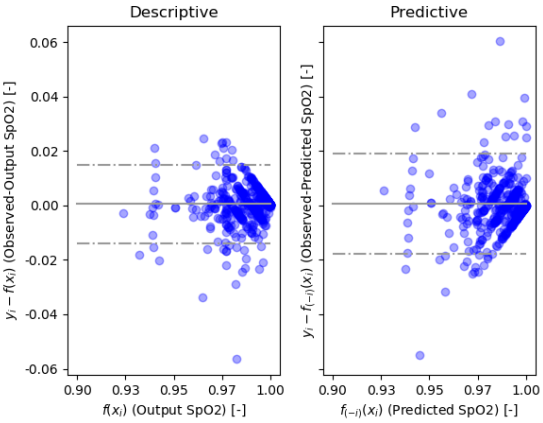

Fig. 4 Bland-Altman analysis for descriptive and predictive modeling. For descriptive modeling (left) the median absolute difference was -0.0005 SpO2 with 95% LoA from -0.0149 to 0.0140 SpO2. For predictive modeling (right) the median absolute difference was -0.0005 SpO2 with 95% LoA from -0.0189 to 0.0179 SpO2

dure should be used with care when circumstance only allows for only a few paired measurements. However, further research should be conducted to determine the predictive capability of the procedure when using measurements with less error.

The procedure described here measures etO2 as a non-invasive representation of PaO2. These two measurements have been shown to agree well [16] in healthy patients with minimal alveolar-arterial (A-a) oxygen gradient. However, these measurements may not yield accurate oxygen saturation response in patient populations with significant A-a gradient. For these populations, oxygen saturation and partial pressure of oxygen measurements acquired by arterial blood gas analysis should be used instead. Conveniently the procedure described here does not require any adjustment to facilitate these type of measurements.

The procedure also measures SpO2 to represent SHbO2. Although SpO2 measurement is less invasive, it has a reported accuracy of ± 2-3% compared with SHbO2. This accuracy was not considered in the present research and may have affected the best-fit parameters, particularly K. If for example, the pulse oximeter reported a SpO2 of 98% at 100% SHbO2, the procedure may have determined the best-fit value of K to be 0.98. With this in consideration, the accuracy of SpO2 may in part have affected the range of K values observed in this study.

Future directions for this research would be to combine the procedure with existing models [8,10] to simulate and predict oxygen saturation and time to desaturation in patients with varying levels of respiratory drive. Predicting the course of SpO2 for a given amount of time could help explore and experiment with simulations on different clinical scenarios that may not be safe to study in volunteers or patients.

5 Conclusion

In summary, this paper has demonstrated and tested a procedure for determining patient-specific pulse oxygen saturation response. The procedure was able to determine best-fit parameters that resulted in significantly improved fit when compared to using standard parameter values. These best-fit parameters increased the coefficient of determination R^2 in all cases.

Acknowledgements This work was supported by a Utah Space Grant Consortium Graduate Research Fellowship (K.M.B.) and Dynasthetics, LLC.

Compliance with Ethical Standards

Funding
This study was partially funded by Dynasthetics, LLC

Conflict of Interest:
Kyle Burk: Dynasthetics, LLC
Joseph Orr: Dynasthetics, LLC

Ethical approval
All procedures performed in studies involving human participants were in accordance with the ethical standards of the institutional and/or national research committee and with the 1964 Helsinki declaration and its later amendments or comparable standards.
Informed consent was obtained from all individual participants included in the study.
This article does not contain any studies with animals performed by any of the authors.

References

1. Applegate, R.L., II, I.L.D., Wells, B., Juma, D., Applegate, P.M.: The relationship between oxygen reserve index and arterial partial pressure of oxygen during surgery. Anesthesia and analgesia **123**(3), 626 (2016)
2. Averick, B.M., Carter, R.G., Xue, G.L., More, J.: The minpack-2 test problem collection. Tech. rep., Argonne National Lab., IL (United States) (1992)
3. Berg, J.M., Tymoczko, J.L., Stryer, L.: Hemoglobin transports oxygen efficiently by binding oxygen cooperatively. NY: WH Freeman & Co (2002)
4. Brockway, J., Hay Jr, W.W.: Prediction of arterial partial pressure of oxygen with pulse oxygen saturation measurements. The Journal of pediatrics **133**(1), 63–66 (1998)
5. Buerk, D.G., Bridges, E.W.: A simplified algorithm for computing the variation in oxyhemoglobin saturation with ph, pco2, t and dpg. Chemical Engineering Communications **47**(1-3), 113–124 (1986)
6. Collins, J.A., Rudenski, A., Gibson, J., Howard, L., O'Driscoll, R.: Relating oxygen partial pressure, saturation and content: the haemoglobin–oxygen dissociation curve. Breathe **11**(3), 194–201 (2015)

7. Dash, R.K., Korman, B., Bassingthwaighte, J.B.: Simple accurate mathematical models of blood hbo2 and hbco2 dissociation curves at varied physiological conditions: evaluation and comparison with other models. European journal of applied physiology **116**(1), 97–113 (2016)
8. Farmery, A., Roe, P.: A model to describe the rate of oxyhaemoglobin desaturation during apnoea. British journal of anaesthesia **76**(2), 284–291 (1996)
9. Gomez-Cambronero, J.: The oxygen dissociation curve of hemoglobin: bridging the gap between biochemistry and physiology. Journal of chemical education **78**(6), 757 (2001)
10. Hardman, J.G., Wills, J.S., Aitkenhead, A.R.: Factors determining the onset and course of hypoxemia during apnea: an investigation using physiological modelling. Anesthesia & Analgesia **90**(3), 619–624 (2000)
11. Hay, W.W., Brockway, J.M., Eyzaguirre, M.: Neonatal pulse oximetry: accuracy and reliability. Pediatrics **83**(5), 717–722 (1989)
12. Hemmings, H.C., Hopkins, P.M.: Foundations of anesthesia: basic sciences for clinical practice. Elsevier Health Sciences (2006)
13. Hsia, C.C.: Respiratory function of hemoglobin. New England Journal of Medicine **338**(4), 239–248 (1998)
14. Jones, E., Oliphant, T., Peterson, P., et al.: SciPy: Open source scientific tools for Python (2001–). URL http://www.scipy.org/. Online; accessed 01/01/2019
15. Leow, M.K.S.: Configuration of the hemoglobin oxygen dissociation curve demystified: a basic mathematical proof for medical and biological sciences undergraduates. Advances in physiology education **31**(2), 198–201 (2007)
16. Myles, P., Heap, M., Langley, M.: Agreement between end-tidal oxygen concentration and the alveolar gas equation: pre and post cardiopulmonary bypass. Anaesth Intensive Care **21**, 240–1 (1993)
17. Næraa, N., Boye, E.: The influence of simultaneous, independent changes in ph and carbon dioxide tension on the in-vitro oxygen tension-saturation relationship of human whole blood. Acta Anaesthesiologica Scandinavica **6**, 20–20 (1962)
18. Severinghaus, J.: Oxyhemoglobin dissociation curve correction for temperature and ph variation in human blood. Journal of applied physiology **12**(3), 485–486 (1958)
19. Siggaard-Andersen, O., Salling, N.: Oxygen-linked hydrogen ion binding of human hemoglobin. effects of carbon dioxide and 2, 3-diphosphoglycerate. ii. studies on whole blood. Scandinavian journal of clinical and laboratory investigation **27**(4), 361–366 (1971)
20. Siggaard-Andersen, O., Wimberley, P., Göthgen, I., Siggaard-Andersen, M.: A mathematical model of the hemoglobin-oxygen dissociation curve of human blood and of the oxygen partial pressure as a function of temperature. Clinical chemistry **30**(10), 1646–1651 (1984)